# On Static and Dynamic Heterogeneities in Water[†]

### Emilia La Nave and Francesco Sciortino*

*Dipartimento di Fisica and INFM Udr and CRS-SOFT: Complex Dynamics in Structured Systems, Università di Roma "La Sapienza", Piazzale Aldo Moro 2, I-00185 Roma, Italy*

We analyze differences in dynamics and in properties of the sampled potential energy landscape between different equilibrium trajectories, for a system of rigid water molecules interacting with a two-body potential. On entering in the supercooled region, differences between different realizations increase and survive even when particles have diffused several time their average nearest neighbor distance. We observe a strong correlation between the mean square displacement of the individual trajectories and the average energy of the sampled landscape.

## I. Introduction

The potential energy landscape (PEL)[1,2] is the surface generated by the potential energy of a system. In the case of a system composed by $N$ rigid molecules, it is a highly complex surface defined in a $6N$ dimensional space. In recent years, numerical studies,[3–11] boosted by the increased computational resources, have attempted to quantify the statistical properties of this surface (for example, quantifying the distribution in energy of specific points of the surface, like local minima and saddles) in the attempt to develop a thermodynamic description fully based on PEL properties. This line of thinking, pioneered by Frank Stillinger and co-workers,[12] has been very fruitful in the study of supercooled liquids, both in equilibrium[4,5,8,13] and in out-of equilibrium conditions.[14–17] Stillinger's formalism builds on the idea that the PEL surface can be partitioned into disjoint basins. A basin is unambiguously defined as the set of points in configuration space connected to the same local minimum—named an inherent structure (IS)—via a steepest descent trajectory. In this respect, the PEL's statistical properties entering in the evaluation of the partition function are the number, shape, and depth of the PEL basins. For its conceptual simplicity and its strict connection with a numerical implementation, the PEL formalism has become one of the modern tools to interpret and analyze simulation data.

Water, due to its intrinsic interest as the liquid of life, has been extensively studied in computer simulations. Models have been developed that are able to reproduce qualitatively the thermodynamic and dynamic anomalies of this liquid.[18–20] Indeed, the thermodynamics of water is characterized by a line of isobaric density maxima and compressibility minima. Its specific heat $C_p$ increases on cooling.[21,22] Recent studies have attempted to connect the thermodynamic anomalies to the presence of a line of first order transition between two liquid structures, eventually ending in a second-order critical point.[23,24] The dynamics of water also shows anomalies. The diffusion coefficient decreases as pressure is increased up to a maximum value (approximately 400 MPa[25]) at room temperature. For greater pressures, the dynamics of water becomes progressively slower, as expected for simple liquids.

Water simulations have been among the first to be scrutinized using the methods developed by Stillinger[4,6,26–30] in the attempt to clarify differences in local structures and relations between structural properties and dynamics. More recently, extensive studies of the PEL properties have been published, providing a detailed description of the landscape properties of several models of water.[6,31–34] Within the PEL formalism, attempts have also been presented in the direction of connecting thermodynamic properties (like the number of explored minima or the number of diffusive directions in the PEL) to dynamics.[4,8,35–43] The outcome of these works, and related studies on different models of glass forming liquids, suggests a strong connection between dynamics and landscape properties. Still, the interpretation schemes require fitting parameters whose physical interpretation is often unclear. As an example, it has been shown that $\ln(D)$ is consistent with a $1/(TS_{conf})$ dependence[4,5,8,13,44] ($S_{conf}$ being the configurational entropy) but no understanding of the proportionality coefficient in term of PEL properties has been reported.[45]

In this article we report analysis of distinct equilibrium trajectories of a system of 216 water molecules interacting via a two-body potential. The novel aspect is the possibility of comparing a large number of independent trajectories (more than 100 for each state point) for a large number of state points. Each of these (previously equilibrated) independent trajectories last more than 20 ns, at which time—even at the slowest studied temperature—the average displacement of the molecule is longer than three nearest neighbors. The analysis of this set of data shows that, though individually each trajectory appears to be to a very good approximation a diffusive trajectory (i.e., with a mean square displacement which increases linearly with time), different realizations are characterized by apparent values of the diffusion coefficient that differ by more than 1 order of magnitude, a clear evidence of dynamic heterogeneities. We also show that differences in dynamics are strongly coupled with the location of the system on the PEL, providing evidence that dynamic heterogeneities are related to inhomogeneities in the local basin energies. For completeness, we briefly discuss the distribution of IS energies for this model and the temperature and density ($\rho$) dependence of the diffusion coefficient, presenting new data with significantly improved statistics.

## II. Simulation Details

We analyze molecular dynamics trajectories of a system composed of 216 rigid water molecules in the (NVE) ensemble. Molecules interact via the widely studied two-body simple point

---

charge extended (SPC/E) model.[18] The integration step is 1 fs, and long range interactions are taken into account using the reaction field method. Dynamics and thermodynamics properties for the SPC/E model have been extensively studied in the past[46] over a wide range of temperatures and densities. Analysis of the statistical properties of the potential energy landscape have also been characterized.[4,6,31−34] Here we analyze a large set of data, on the basis of five different temperatures in supercooled states and nine different densities, from 0.9 to 1.4 g/cm³. At each state point, we analyze equilibrated trajectories of more than 100 independent realizations, to both reduce significantly the numerical error and to estimate the self-averaging properties of this model for different $T$ and $\rho$. Each trajectory covers a time interval of about 20 ns. Potential energy landscape properties have been based on the analysis of the inherent structures, which has been calculated using a standard conjugate gradient minimization algorithm with a $10^{-15}$ tolerance.[47]

### III. IS Energies: the Random Energy Model

A quantification of the statistical properties of the potential energy landscape, i.e., the distribution of basin's depth and shapes, for the SPC/E model of water has been recently reported.[34] It has been shown that the number $\Omega(e_{IS})\,de_{IS}$ of distinct basins of energy depth $e_{IS}$ between $e_{IS}$ and $e_{IS} + de_{IS}$ follows a Gaussian distribution,

$$\Omega(e_{IS})\,de_{IS} = e^{\alpha N}\frac{e^{-(e_{IS}-E_o)^2/2\sigma^2}}{\sqrt{2\pi\sigma^2}}\,de_{IS} \qquad (1)$$

where $e^{\alpha N}$ is the total number of distinct basins of the PEL for the system of $N$ molecules, $E_0$ is the energy scale of the distribution, and $\sigma^2$ is the variance. The coefficients $\sigma$, $E_o$, and $\alpha$ depend only on the system density. The corresponding probability distribution $P(e_{IS},T)$ of sampling an IS of depth $e_{IS}$ in equilibrium at temperature $T$ is given by

$$P(e_{IS},T) = \frac{\Omega(e_{IS})e^{-\beta[e_{IS}+f_{vib}(T,e_{IS})]}}{\int P(e_{IS},T)\,de_{IS}} \qquad (2)$$

where $\beta = 1/kT$ and $f_{vib}(T,e_{IS})$ is the basin free energy.[3,5] The hypothesis of a Gaussian form for $\Omega(e_{IS})$, together with the assumption of an $e_{IS}$ independence of the basin anharmonicities implies (i) that the $T$ dependence of the average IS energy $\langle e_{IS}(T)\rangle$, at constant volume, is linear as a function of $T^{-1}$,[48−50] that is

$$\langle e_{IS}(T)\rangle = A + \frac{B}{T} \qquad (3)$$

where the coefficients $A$ and $B$ depend only on $\rho$ and can be expressed in term of landscape properties,[50] and (ii) that the probability distribution $P(e_{IS},T)$ is Gaussian with a $T$-independent variance.[48−54]

To provide evidence of this behavior, we report in Figure 1 $\langle e_{IS}(T)\rangle$ at all studied densities. In all cases, in the investigated $T$ range, the expected $T^{-1}$ dependence holds. Nevertheless, two breakdowns of eq 3 are expected outside the investigated $T$ region. At high $T$, due to the increasing importance of the anharmonic contribution to the basin free energy[49] and at low $T$ due to possible presence of non-Gaussian corrections to the $e_{IS}$ probability distribution (eq 1). The low $T$ region cannot be numerically studied due to the huge increase of the relaxation times. Figure 2 shows the $\rho$ dependence of $A$ and $B$ (which have well-defined landscape interpretations[50]). As a first
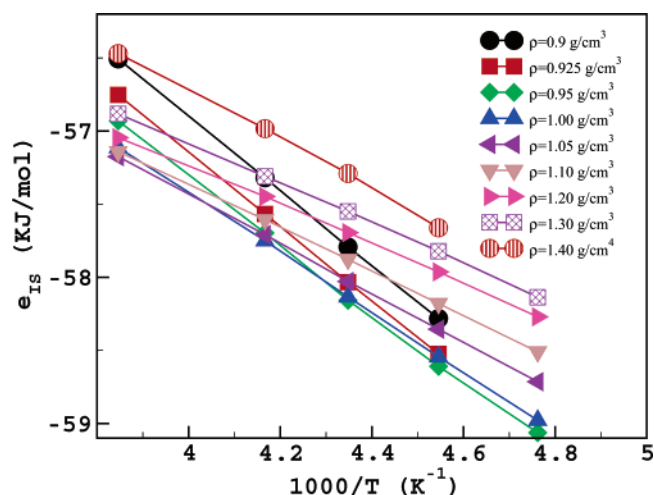


**Figure 1.** Temperature dependence of the average $\langle e_{IS}\rangle(T)$ for all investigated densities.
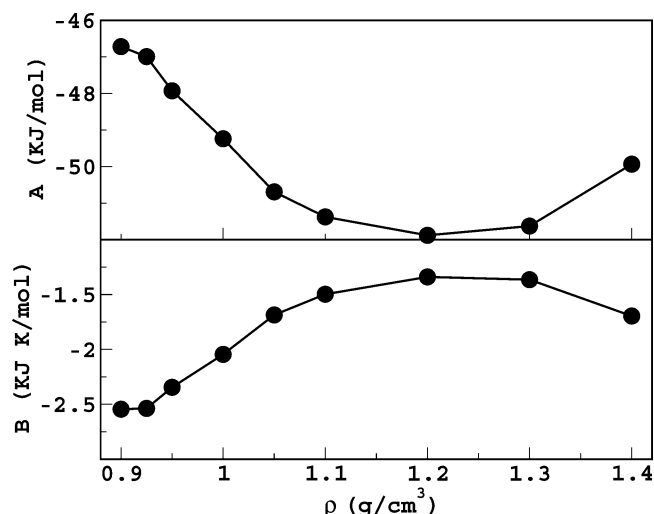


**Figure 2.** Density dependence of the fitting parameters $A$ and $B$ in eq 3.

approximation (but see ref 49 for a more precise discussion), $A$ is related to $E_0$ and $B$ to $\sigma^2$.

The large available data set allows us to evaluate $P(e_{IS},T)$ and test the prediction of a Gaussian form of $P(e_{IS},T)$. Figures 3a and 4a show $P(e_{IS},T)$ respectively for $\rho = 0.95$ g/cm³ and $\rho = 1.00$ g/cm³. The figures show that the shape of the distribution is, to a first approximation, Gaussian and that the variance of the distribution only weakly increases with $T$, as can be inferred by the small change of the heigh of the distribution with $T$.

The availability of 100 independent realizations allows us to study also the distribution of $P(\langle e_{IS}\rangle_i,T)$, defined as the distribution of the average depth sampled in each independent trajectory $i$ in the simulated 20 ns time interval. In this case, of course, each distribution is evaluated only over 100 points. If the length of each trajectory is sufficiently long, so that the system is able to sample all basins that are statistically relevant at that temperature, the distribution should be peaked around the average of $P(e_{IS},T)$, with a small variance. Figures 3b and Figure 4b show that this is the case only at the higher $T$. On cooling, the relaxation time of the system increases and, within the time of the simulation, the system retains memory of the initial basin. It is important to observe that the distribution becomes very asymmetric, developing a long tail at low basin energies. This may suggest a strong relation between depth of the explored
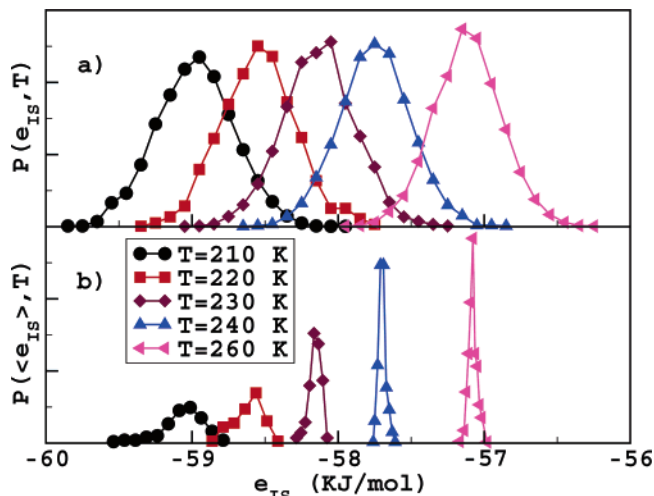
Static and Dynamic Heterogeneities in Water

*J. Phys. Chem. B, Vol. 108, No. 51, 2004* **19665**



**Figure 3.** (a) Probability distribution of the $e_{IS}$ (per molecule) at density $d = 0.95$ g/cm$^3$, for different $T$ values. (b) Probability distribution of $\langle e_{IS} \rangle$, where each average is calculated over one distinct trajectory. Units are arbitrary. Each $P(e_{IS},T)$ is calculated using 5000 points, because from each of the 100 independent trajectories we evaluated 50 different inherent structures, minimizing at intervals equally spaced in time.
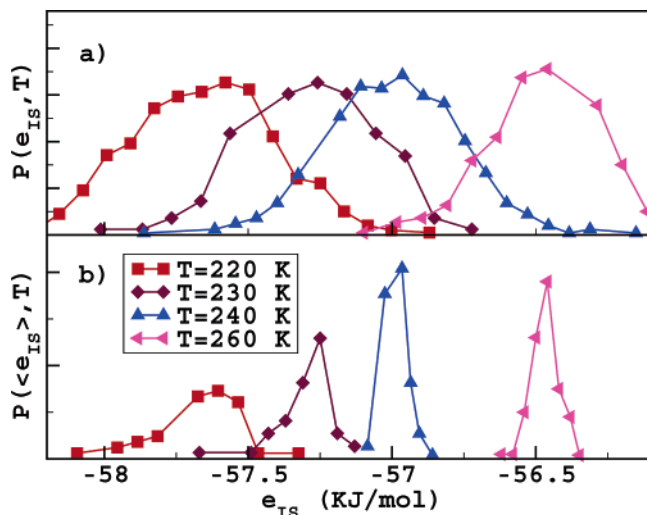


**Figure 4.** Same as Figure 3 for $d = 1.40$ g/cm$^3$.

basin and dynamics, which cannot be attributed to differences in thermal energy, because all different realizations have the same kinetic energy. In particular, the asymmetry in the resulting distribution suggests that configurations starting from low energy basins do not have time to explore phase space sufficiently. It is worth stressing that similar results are observed at all investigated densities. To support this hypothesis, we show in Figure 5 the time evolution of $e_{IS}$ and of the center of mass mean square displacement MSD$_i$ for two different trajectories at the same $T$ and $\rho$. More precisely, the mean square displacement of the trajectory $i$ is defined as

$$\text{MSD}_i = \frac{1}{N}\sum_{j=1}^{N}[\vec{r}_j^{\,CM}(t) - \vec{r}_j^{\,CM}(0)]^2 \qquad (4)$$

where $\vec{r}_j^{\,CM}(t)$ is the location of the center of mass of molecule $j$ in the trajectory $i$ at time $t$. The averaged *MSD* is defined as

$$\text{MSD} = \frac{1}{\mathcal{N}_t}\sum_{i}^{\mathcal{N}_t}\text{MSD}_i \qquad (5)$$



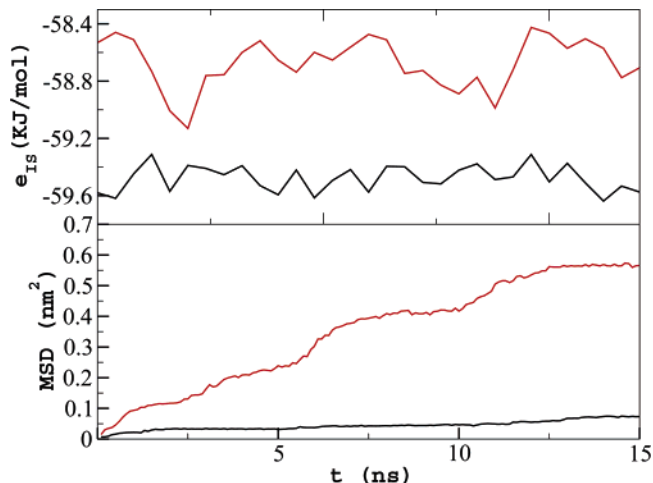**Figure 5.** $e_{IS}$ and the mean square displacement as a function of time for two different trajectory at $T = 210$ K and $\rho = 0.95$ g/cm$^3$.

where $\mathcal{N}_t$ is the number of independent trajectories. The two chosen trajectories differ by the value of $e_{IS}$ at time 0. In the studied $t$ range (nanoseconds), both configurations sample a restricted interval of $e_{IS}$ values. The memory of the energy of the starting basins is preserved during the simulation time. Comparing Figure 5,b, we note that the configuration with large $e_{IS}$ is characterized by a larger MSD.

## IV. Dynamic Heterogeneities

We next focus the attention on dynamic heterogeneities via a study of the mean square displacement of the individual trajectories.[35,55] For each state point $(T, \rho)$ we calculate MSD$_i$ for each of the $\mathcal{N}_t$ trajectories. Figure 6 shows MSD$_i$ for $\rho = 0.95$ g/cm$^3$ at three selected $T$, but similar results are obtained for all the other studied densities. In all cases, no averaging over different time origins is performed. In the figure, the time axis are chosen in such a way that the average MSD at the maximum reported time coincides for all temperatures. A comparison of the spreading of the different realizations at fixed value of the average MSD, for example at the maximum reported time, reveals a clear increase in the fluctuations of the different trajectories on lowering $T$.

To better quantify fluctuations in dynamics and the role of $T$, we calculate the variance of the mean square displacement of different trajectories. More precisely, we evaluate, for each time $t$

$$\sigma_{MSD} = \sqrt{\frac{\sum_{i}(\text{MSD}_i - \text{MSD})^2}{\mathcal{N}_t - 1}} \qquad (6)$$

Figure 7 shows the behavior of the variance $\sigma_{MSD}$ as a function of the average MSD, parametrically in $t$, for several different $T$. This representation, which accounts for the intrinsic effect of the slowing down of the dynamics on cooling by eliminating $t$, confirms that dynamic heterogeneities grow significantly on supercooling. Data in Figure 7 quantify that the spreading of the MSD$_i$ values is much more enhanced at low $T$. The $T$ dependence of the slope of the curves shown in Figure 7 is shown in Figure 8.

It is interesting to compare results reported in Figures 7 and 8 with expectations for a Gaussian random walk process. For this case, the probability of finding the walker after time $t$ at
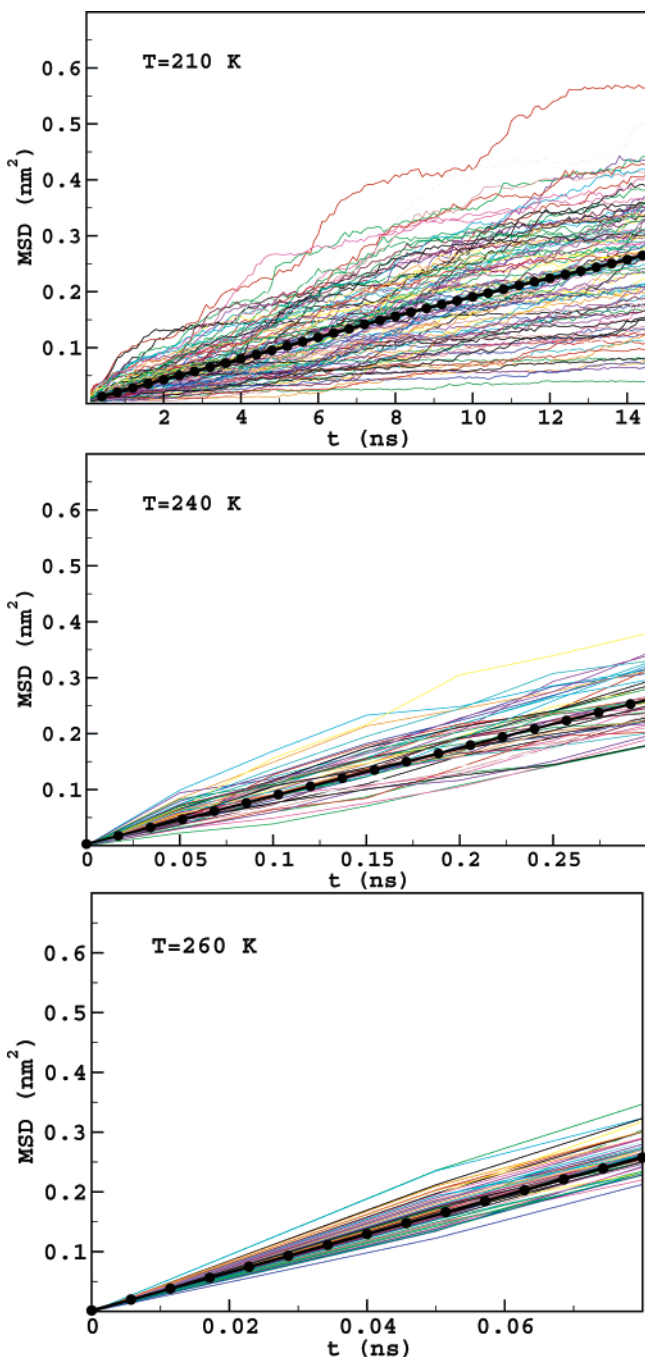
**Figure 6.** Individual mean square displacement for 100 independent realizations at three different temperatures. Filled symbols indicate the MSD averaged over the different realizations. Note that no average over starting time has been performed.

distance $r^2$ from the location at the time origin is

$$P(r^2,t)\, dr^2 = \sqrt{\frac{27}{2\pi}} \frac{\sqrt{r^2}}{\langle r^2(t)\rangle^{3/2}} e^{-3r^2/2\langle r^2(t)\rangle}\, dr^2 \qquad (7)$$

The first and second moments of this distribution are given by

$$\langle r^2 \rangle = \int_0^\infty r^2 P(r^2,t)\, dr^2 = \langle r^2(t)\rangle \qquad (8)$$

and

$$\langle r^4 \rangle = \int_0^\infty r^4 P(r^2,t)\, dr^2 = \frac{5}{3}\langle r^2(t)\rangle^2 \qquad (9)$$
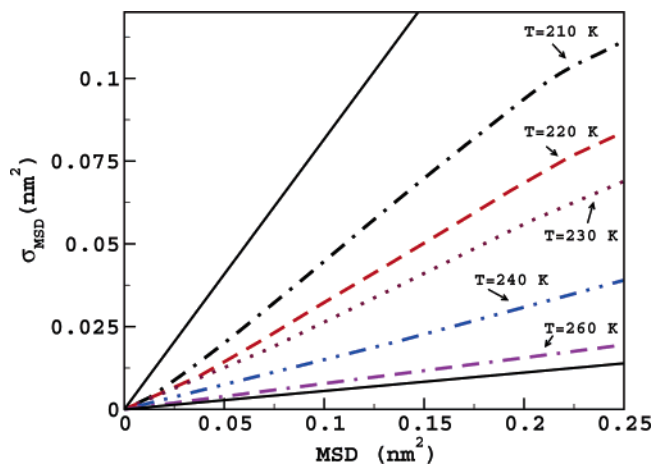


**Figure 7.** Variance $\sigma_{MSD}$ of the MSD as a function of the average MSD for $\rho = 0.95$ g/cm$^3$, for different $T$. The two full lines indicate the two extreme limits provided by eqs 11−12. Note that in water the nearest neighbor distance is 0.28 nm, corresponding to a square displacement of $\approx$0.09 nm$^2$.
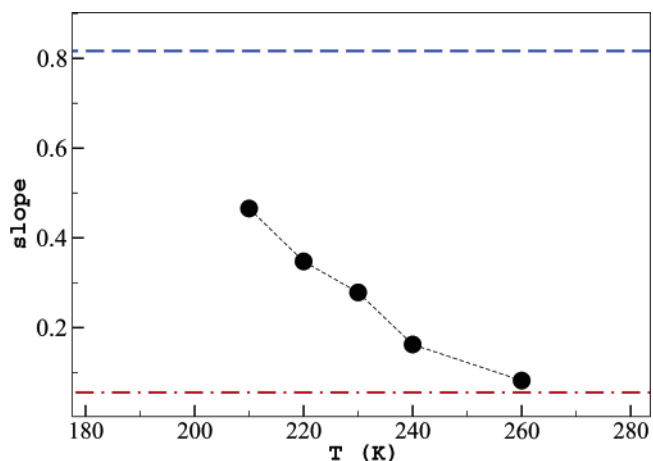


**Figure 8.** Slope of $\sigma_{MSD}$ vs MSD as a function of $T$ for $\rho = 0.95$ g/cm$^3$. The two lines indicate the two extreme limits provided by eqs 11−12.

The variance $\delta$ of $r^2$ between different trajectories of the walker is

$$\delta^2 = \langle (r^2 - \langle r^2\rangle)^2\rangle = \frac{2}{3}\langle r^2(t)\rangle^2 \qquad (10)$$

Hence, a plot of $\delta$ vs $\langle r^2(t)\rangle$ has, for a single Gaussian walker, a slope of $\sqrt{2/3}$, a universal value independent of the diffusion constant. If the dynamics in simulated water could be represented by the dynamics of $N = 216$ independent walker, then $\sigma_{MSD}$ should be related to MSD by the relation

$$\sigma_{MSD} = \sqrt{\frac{2}{3}} \frac{1}{\sqrt{N}} MSD \qquad (11)$$

because each MSD$_i$ would be the sum of $N$ independent Gaussian processes (with a reduction of the variance by a factor $\sqrt{N}$ as compared to the single random walker case). Data in Figures 7 and 8 show that this limit is approached at high $T$.

In another extreme theoretical case, each realization can be considered as a single random Gaussian process (for example, in the limit of strong correlation between all $N$ molecules, or in the limit of one single diffusing molecule). In this limit, the expected relation between $\sigma_{MSD}$ and MSD would be

Static and Dynamic Heterogeneities in Water

*J. Phys. Chem. B, Vol. 108, No. 51, 2004* **19667**

$$\sigma_{MSD} = \sqrt{\frac{2}{3}} MSD \qquad (12)$$

For reference, this limit is also reported in Figures 7 and 8.

Data shown in Figures 7 and 8 show that a crossover from the behavior of eq 11 to the behavior of eq 12 takes place on supercooling. It will be very interesting to study the size, $T$, and $t$ dependence of these effects. Moreover, because each of the equilibrium trajectories of the 216 molecule system can be thought as representative part of a large system, the increase of the variance with decreasing $T$ provides a strong evidence of growing dynamic heterogeneities in the system. In this respect, this set of data, or analogous data for simpler potentials, may become a relevant tool for discriminating between different theories of the glass transitions, in particular between the ones based on facilitated dynamics ideas[56] and trap models.[57,58]

## V. Correlation between Diffusion Coefficient and $e_{IS}$

Bulk dynamic properties of SPC/E water have been previously investigated in detail.[59−63] In particular, PEL inspired studies have investigated the relation between the $T$ and $\rho$ dependence of the diffusion coefficient $D$ and the number of unstable directions in configuration space,[36] as well as the relation between $D$ and the configurational entropy.[4] Figure 9 shows the average diffusion coefficient $D$, evaluated from the MSD long time limit, for several studied density and temperatures. The present set of data improves the precision of previous estimate for the same model.[62] Despite the relatively small $T$ range investigated in this study, $D$ varies over more than 3 orders of magnitudes. It also clearly show that, among all the studied densities, $D$ is largest around density 1.1 g/cm³. When $\rho$ increases, dynamics slow due to the packing effect, whereas when $\rho$ decreases, dynamics slow due to the development of a network of hydrogen bonds.

Most of previous studies on dynamic heterogeneities[64−66] have focused on the dynamics of different subsets of molecules in the same system, raising sometimes the question if the observed results were somehow associated with the chosen rules for identifying slow and fast particles. It is also fairly difficult to correlate properties of the subset of molecules to energetic properties, due to the difficulty of separating unambiguously the single particle energy contributions. In the present approach, heterogeneities are addressed globally, as a fluctuation phenomenon. To better clarify the connection between dynamic and energetic (static) heterogeneities, we correlate the apparent diffusion coefficient of each trajectory with the corresponding average inherent structure. Indeed, it is important to observe that, when each trajectory is averaged over different time origins, the resulting MSD behaves linearly with $t$, such that an apparent trajectory diffusion coefficient $D_i$ can be estimated. Differences in $D_i$ values between different trajectories persist even for time such that molecules have diffused over distances larger than two molecular diameters ($\approx 0.3$ nm being the distance between the center of mass of two nearest neighbor molecules).

Figure 10 shows a plot of the average $D(T)$ as a function $\langle e_{IS}\rangle(T)$ for one selected isochore. It also shows for each trajectory $i$ (at the same $T$ and $\rho$), the apparent diffusion coefficient $D_i$ vs the average sampled $\langle e_{IS}\rangle_i$. While at larger $T$, self-averaging is well accomplished on the time scale of the simulation, at lower $T$, each trajectory—even if diffusive over distances of several molecular diameters—samples only a small part of the statistically relevant configurational space, resulting in a large spreading in the value of $\langle e_{IS}\rangle_i$. Interestingly enough,
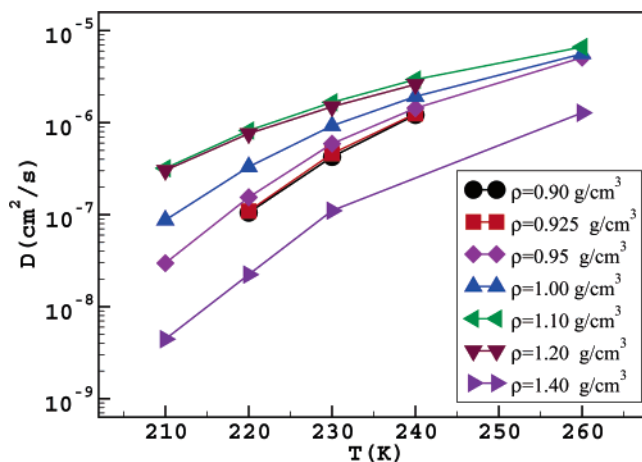


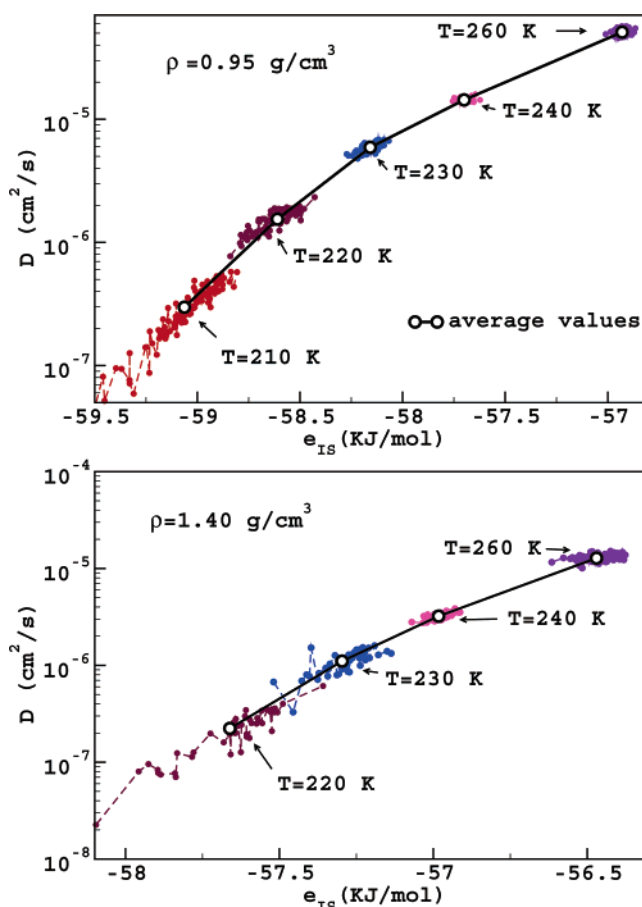**Figure 9.** Average diffusion coefficient $D$ as a function of $T$ for several studied densities.



**Figure 10.** Comparison between the average diffusion coefficient (line with open circles) and the diffusion coefficient of each single trajectory at $\rho = 0.95$ g/cm³ (top panel) and $\rho = 1.40$ g/cm³ (lower panel).

such a spreading in $\langle e_{IS}\rangle_i$ is strongly correlated to the spreading in the $D_i$ values.

The relation between $D_i$ and $\langle e_{IS}\rangle_i$ displayed by the data is not very different from the corresponding relation $D$ vs $\langle e_{IS}\rangle$ for the averaged values. A more detailed study of $D_i$ vs $\langle e_{IS}\rangle_i$ over a smaller grid of temperatures, allowing for overlap of different $(D_i - \langle e_{IS}\rangle_i)$ pairs of points could help sort out the $T$ and $e_{IS}$ roles. Indeed, one could associate each $e_{IS}$ with a precise value of $D(e_{IS})$ and, in analogy with the thermodynamics formalism developed by Stillinger, one could attempt to calculate $D(T)$ as[11]

$$D(T) = \int D(e_{IS})\, \mathscr{F}(e_{IS},T)\, P(e_{IS},T)\, de_{IS} \qquad (13)$$

where $\mathscr{F}(e_{IS},T)$ account for the role of $T$ in dynamics and $P(e_{IS},T)$ is calculated according to Stillinger's PEL formalism. If this goal would be reached, the PEL formalism would become an exceptionally rich tool not only for describing the thermodynamics of supercooled liquids but also their dynamics.

## VI. Conclusion

One of the key features in the slowing down of the dynamics of liquids on approaching supercooled states—i.e., when the dynamics begin to slow significantly as compared to the standard liquid values—is the development of local fluctuations both in static and in dynamic properties. Current computational resources allow us to start looking carefully into this problem, by performing an analysis of these fluctuations.[54] These approaches, compared to the corresponding studies of the average properties, are complicated by the interplay between space and time. The data reported in this article, more than providing conclusive answers, hopefully clarify the richness of this type of analysis and should stimulate further studies focusing on the time and space evolution of these fluctuations. The presented preliminary analysis reported here clearly shows that the role of fluctuations significantly grows on cooling. Comparing fluctuations in dynamics at fixed mean square displacement (Figure 7), we have detected a progressive increase of the fluctuations on cooling, already in the region of early supercooling, where MCT appears to provide a consistent description of the dynamics.[60] Interestingly, self-averaging properties appear to set in only after molecules have diffused several particle diameters. This finding not only clarifies the difficulty of calculating reliable values for dynamical quantities in deep supercooled states but calls attention on the fact that a complete decorrelation of the system requires, at low $T$, rearrangements that extend much beyond the first neighbor shell.

We have also observed a clear correlation between the apparent diffusion coefficient of the individual realizations and depth of the sampled PEL (Figure 10). Again, the comparison of different trajectories, all at the same temperature, helps in eliminating trivial (but a priori unknown) thermal effect, highlighting the connection between dynamics and IS energies. In this respect, one goal of future studies should be the development of a (size dependent) dynamical histogram reweighting formalism, conceptually similar to the one used to calculate the density of states, from which the relation $D(e_{IS})$ could be extracted. This would allow us to sort out the role of $T$ and $e_{IS}$ in dynamics, and to describe in terms of PEL properties not only the thermodynamics of supercooled liquids but also their dynamics.

## References and Notes

(1) Wales, D. J. *Energy Landscapes*; Cambridge University Press: Cambridge, U.K., 2003.

(2) Debenedetti, P. G.; Stillinger, F. H. *Nature* **2001**, *410*, 259.

(3) Sciortino, F.; Kob, W.; Tartaglia, P. *Phys. Rev Lett.* **1999**, *83*, 3214.

(4) Scala, A.; Starr, F. W.; La Nave, E.; Sciortino, F.; Stanley, H. E. *Nature* **2000**, *406*, 166.

(5) Sastry, S. *Nature* **2001**, *409*, 164.

(6) Starr, F. W.; Sastry, S.; La Nave, E.; Scala, A.; Stanley, H. E.; Sciortino, F. *Phys. Rev. E* **2001**, *63*, 041201.

(7) Speedy, R. J. *J. Chem. Phys.* **2001**, *114*, 9069.

(8) Mossa, S.; La Nave, E.; Stanley, H. E.; Donati, C.; Sciortino, F.; Tartaglia, P. *Phys. Rev. E* **2002**, *65*, 041205−1.

(9) Wales, D. J. *Science* **2001**, *293*, 2067.

(10) Lacks, D. J. *Phys. Rev. Lett.* **1998**, *80*, 5385.

(11) Doliwa, B.; Heuer, A. *Phys. Rev. Lett.* **2003**, *91*, 235501.

(12) Stillinger, F. H.; Weber, T. A. *Phys. Rev. A* **1982**, *25*, 978. Stillinger, F. H.; Weber, T. A. *Science* **1984**, *225*, 983. Stillinger, F. H. *Science* **1995**, *267*, 1935.

(13) Saika-Voivod, I.; Poole, P. H.; Sciortino, F. *Nature (London)* **2001**, *412*, 514.

(14) Sciortino, F.; Tartaglia, P. *Phys. Rev. Lett.* **2001**, *86*, 107.

(15) Crisanti, A.; Ritort, F. *Europhys. Lett.* **2000**, *52*, 640.

(16) Mossa, S.; La Nave, E.; Sciortino, F.; Tartaglia, P. *Eurphys. J. B* **2002**, *30*, 351.

(17) Shell, M. S.; Debenedetti, P. G.; La Nave, E.; Sciortino, F. *J. Chem. Phys.* **2003**, *118*, 8821.

(18) Berendsen, H. J. C.; Grigera, J. R.; Stroatsma, T. P. *J. Phys. Chem.* **1987**, *91*, 6269.

(19) Mahoney, M. W.; Jorgensen, W. L. *J. Chem. Phys.* **2000**, *112*, 8910; *ibid* **2001**, *114*, 363.

(20) Stillinger, F. H.; Rahaman, A. *J. Chem. Phys.* **1974**, *60*, 1545.

(21) Angell, C. A. In *Water: A Comprehensive Treatise*;. Franks, F., Ed.; Plenum: New York, 1982; Vol. 7, pp 1−81.

(22) Debenedetti, P. G. *Metastable liquids*; Princeton University Press: Princeton, NJ, 1997.

(23) Poole, P. H.; Sciortino, F.; Essmann, U.; Stanley, H. E. *Nature* **1992**, *360*, 324.

(24) Ponyatovsky, E. G.; Sinitsyn, V. V.; Pozdnyakova, T. A. *JEPT Lett.* **1994**, *60*, 360.

(25) Prielmeier, F. X.; Lang, E. W.; Speedy, R. J.; Ludemann, H. D. *Phys. Rev. Lett.* **1987**, *59*, 1128.

(26) Stillinger, F. H.; Weber, T. A. *J. Phys. Chem.* **1983**, *87*, 2833.

(27) Ohmine, I.; Tanaka, H.; Wolynes, P. G. *J. Chem. Phys.* **1988**, *89*, 5852.

(28) Sasai, M.; Ohmine, I.; Ramaswamy, R. *J. Chem. Phys.* **1992**, *96*, 3045.

(29) Sciortino, F.; Geiger, A.; Stanley, H. E. *J. Chem. Phys.* **1992**, *96*, 3857.

(30) Sciortino, F.; Geiger, A.; Stanley, H. E. *Nature* **1991**, *354*, 218.

(31) Roberts, C. J.; Debenedetti, P. G.; Stillinger, F. H. *J. Phys. Chem. B* **1999**, *103*, 10258.

(32) Giovambattista, N.; Stanley, H. E.; Sciortino, F. *Phys. Rev. Lett.* **2003**, *91*, 115504.

(33) La Nave, E.; Sciortino, F.; Scala, A.; Stanley, H. E.; Starr, F. W. *Eur. Phys. J. E* **2002**, *9*, 233.

(34) Sciortino, F.; La Nave, E.; Tartaglia, P. *Phys. Rev. Lett.* **2003**, *91*, 155701.

(35) Keyes, T. *J. Chem. Phys.* **1994**, *101*, 5081.

(36) La Nave, E.; Scala, A.; Starr, F.; Stanley, H. E.; Sciortino, F. *Phys. Rev. Lett.* **2000**, *84*, 4605.

(37) Angelani, L.; Di Leonardo, R.; Ruocco, G.; Scala, A.; Sciortino, F. *Phys. Rev. Lett.* **2000**, *85*, 5356.

(38) La Nave, E.; Stanley, H. E.; Sciortino, F. *Phys. Rev. Lett.* **2002**, *88*, 035501.

(39) Heuer, A. *Phys. Rev. Lett.* **1997**, *78*, 4051. Büchner, S.; Heuer, A. *Phys. Rev. E* **1999**, *60*, 6507.

(40) Broderix, K.; Bhattacharya, K. K.; Cavagna, A.; Zippelius, A.; Giardina, I. *Phys. Rev. Lett.* **2000**, *85*, 5360.

(41) Doliwa, B.; Heuer, A. *Phys. Rev. E* **2003**, *67*, 030501.

(42) Schrøder, T. B.; Sastry, S.; Dyre, J. C.; Glotzer, S. C. *J. Chem. Phys.* **2000**, *112*, 9834.

(43) Fynewever, H.; Perera, D.; Harrowell, P. *J. Phys. Condens. Mater.* **2000**, *12*, A399.

(44) De Michele, C.; Sciortino, F.; Coniglio, A. cond-mat 0405282 2004.

(45) Ruocco, G.; Sciortino, F.; Zamponi, F.; De Michele, C.; Scopigno, T. *J. Chem. Phys.* **2004**, *120*, 10666.

(46) Roberts, C. J.; Debenedetti, P. G.; Stillinger, F. H. *J. Phys. Chem. B* **1999**, *103*, 10258.

(47) Numerical recepies, http://www.nr.com/nronline5#5.html.

(48) Sastry, S.; Debenedetti, P. G.; Sciortino, F.; Stanley, H. E. *Phys. Rev. E* **1996**, *53*, 6144.

(49) La Nave, E.; Sciortino, F.; Tartaglia, P.; De Michele, C.; Mossa, S. *J. Phys: Condens. Matter* **2003**, *15*, 1.

(50) La Nave, E.; Mossa, S.; Sciortino, F. *Phys. Rev. Lett.* **2002**, *88*, 225701[1].

(51) Sasai, M. *J. Chem. Phys.* **2003**, *118*, 10651.

(52) Derrida, B. *Phys. Rev. B* **1981**, *24*, 2613.

(53) Keyes, T.; Chowdhary, J.; Kim, J. *Phys. Rev. B* **2002**, *66*, 051110.

(54) Saika-Voivod, I.; Sciortino, F. *Phys. Rev. E* **2004**, *70*, 041202.

(55) Li, W. X.; Keyes, T. *J. Chem. Phys.* **1999**, *111*, 328.

(56) Garrahan, J. P.; Chandler, D. *Phys. Rev. Lett.* **2002**, *89*, 035704.

(57) Dyre, J. C. *Phys. Rev. Lett.* **1987**, *58*, 792. Dyre, J. C. *Phys. Rev. B* **1995**, *51*, 12276.

Static and Dynamic Heterogeneities in Water

*J. Phys. Chem. B, Vol. 108, No. 51, 2004* **19669**

(58) Bouchaud, C. M.; Bouchaud, J.-P. *J. Phys. A: Math. Gen.* **1996**, *29*, 3847−3869, and references therein.

(59) Sciortino, F.; Gallo, P.; Tartaglia, P.; Chen, S. H. *Phys. Rev. E* **1996**, *54*, 6331. Gallo, P.; Sciortino, F.; Tartaglia, P.; Chen, S. H. *Phys. Rev. Lett.* **1996**, *76*, 2730.

(60) Fabbian, L.; Latz, A.; Schilling, R.; Sciortino, F.; Tartaglia, P.; Theis, C. *Phys. Rev. E* **1999**, *60*, 5768.

(61) Harrington, S.; Poole, P. H.; Sciortino, F.; Stanley, H. E. *J. Chem. Phys.* **1997**, *107*, 7443.

(62) Starr, F. W.; Sciortino, F.; Stanley, H. E. *Phys. Rev. E* **1999**, *60*, 6757.

(63) Sciortino, F. *Chem. Phys.* **2000**, *258*, 307.

(64) Donati, C.; Douglas, J. F.; Kob, W.; Plimpton, S. J.; Poole, P. H.; Glotzer, S. C. *Phys. Rev. Lett.* **1998**, *80*, 2338.

(65) Kob, W.; Donati, C.; Plimpton, S. J.; Poole, P. H.; Glotzer, S. C. *Phys. Rev. Lett.* **1997**, *79*, 2827−2830.

(66) Giovambattista, N.; Buldyrev, S. V.; Starr, F. W.; Stanley, H. E. *Phys. Rev. Lett.* **2003**, *90*, 085506.